5-1-2020

ELECTRONIC COOLING OF AIRBUS HELICOPTER CONTROL PANEL

Cristobal Garces

ELECTRONIC COOLING OF AIRBUS HELICOPTER CONTROL PANEL

by

CRISTOBAL CHAUNCE GARCES

Presented to the Faculty of the Honors College of

The University of Texas at Arlington in Partial Fulfillment

of the Requirements

for the Degree of

HONORS BACHELOR OF SCIENCE IN MECHANICAL ENGINEERING

THE UNIVERSITY OF TEXAS AT ARLINGTON

May 2020

ACKNOWLEDGMENTS

I would like to thank my team members, Anna Dorack, Erin Hollingsworth, James Nguyen, Miranda Hucaby, and Phimvaly Sarawichitr for their unparalleled work on the project. I would also like to express my gratitude for our faculty advisor, Dr. Dereje Agonafer, and his graduate students, Uschas Chowdury and Pardeep Shahi for their guidance throughout the year. Finally, I would like to recognize our sponsors at Airbus for providing us the information to complete our design tasks and giving their insight into how to approach various aspects of this project.

May 6, 2020

ABSTRACT

ELECTRONIC COOLING OF AIRBUS CONTROL PANEL

Cristobal Garces, B.S. Mechanical Engineering

The University of Texas at Arlington, 2020

Faculty Mentor: Raul Fernandez

The technological necessities of the modern helicopter are always evolving. However, helicopters themselves are rarely modified to compensate for these new technologies. Because of this, as more precise electrical equipment replaces archaic analog instruments, unexpected issues arise in these older vehicles that were not present before. Temperatures within the helicopter cabin and control panel reach dangerous levels, causing extreme discomfort for the pilot as well as causing equipment failure. To amend this issue, cooling methods must be employed to prevent failure of instrumentation which will also reduce temperatures in the cabin. The primary goal of the project is to create a cooling method that provides the most cooling to the control panel. This report summarizes the computational fluid dynamic simulation results completed and analyzed by the Honors Student, which include various cooling methods that will be reported to Airbus.

TABLE OF CONTENTS

LIST OF ILLUSTRATIONS

LIST OF TABLES

CHAPTER 1

INTRODUCTION

1.1 Problem Statement

The Airbus H125 Helicopter was developed in the 1970s for civil services. This model has proved to be reliable and has thus continued to see use to this day. As equipment transitions from analog to digital and more electronics are added to the helicopter's control panel, cooling becomes more of a concern. The equipment has a critical temperature threshold that when exceeded, will cause them to cease proper functionality. Malfunctioning/failed equipment needs no explanation regarding the severity of this issue.

Figure 1.1: Airbus H125M in Flight (1)

The project presented to us can be simplified to an electronic cooling problem. Cooling, like most engineering topics, is a combination of many disciplines and studies. Thermodynamics, heat transfer, and fluid dynamics are just a few areas of study that will be utilized in this project. Rather than addressing this complex problem through hand calculations, ANSYS Icepak, a computational fluid dynamic software, will be employed.

Utilizing Icepak allows us to create a representative model of the helicopter cabin and implement various cooling techniques without the need for physical experimentation.

Methods to provide sufficient cooling include adding perforations to the hood of the control panel, which allows heated air to escape through natural convection, and adding fans, which will cool the control panel through forced convection. Airbus had previously experimented with several cooling strategies with fans that failed to deliver desired results. However, the fan cooling methods described in this report proves promising and will be discussed in further detail in later sections. The only current cooling method used on the helicopter is through ram air intake valve cooling located at the nose of the vehicle. This cooling method provides cooling only when the helicopter is in motion, where outside air in brought into the control panel. Some of this intake air is also redirected toward the pilot.

1.2 Airbus Provided Data

Airbus had performed and provided data on the internal temperatures of the H125 Helicopter during various stages of flight. These results can be seen in Table 1.1 where the electrical equipment positions can be seen in Figure 1.2. The temperatures reported must be extrapolated to an outside air temperature, OAT, of an assumed 50 °C. Extrapolating the results adds an additional 20 °C to all data points. Airbus had found that the internal air temperatures are at their highest during hovering, where there is no motion is taking place. The highest temperature, which is bolded in Table 1.1 is 30.4 °C, which is 50.4 °C following the extrapolation. These temperatures were recorded using temperature probes at different locations within the control panel. This data was used to validate Icepak models so that cooling techniques applied will accurately reflect any real implementations into the

control panel. The goal of the project is not to completely replicate the experimental data in Icepak, but rather achieve a functioning proof of concept that provides the most cooling.

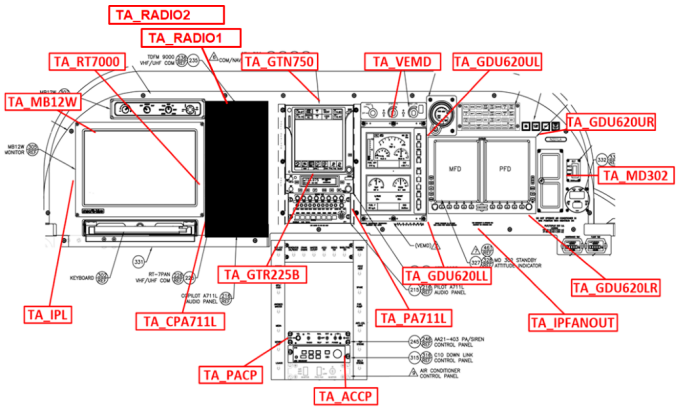

Figure 1.2: Control Panel and Temperature Probe Locations

Table 1.1: Equipment Probe Temperatures

Parameter	Measured [°C]					
	Heat Soak	Hover	0.97 σ	0.89 σ	0.80 σ	SD
TA_CABIN	35.9	18.0	12.6	11.1	8.7	11.6
TA_OAT	11.3	9.2	6.6	6.3	3.5	9.1
TA_MB12W	39.8	23.2	16.9	16.4	14.0	14.0
TA_IPL	32.2	20.5	15.3	14.0	12.2	14.6
TA_RADIO1	50.0	25.4	18.8	17.6	15.3	16.8
TA_RADIO2	34.6	21.0	15.5	14.5	12.9	14.6
TA_PACP	26.6	25.8	25.6	25.0	24.0	22.4
TA_AACP	27.2	23.3	23.0	22.0	20.5	19.4
TA_GDU620LL	33.0	23.8	19.5	17.9	15.9	16.4
TA_GDU620LR	34.2	21.0	15.5	13.9	0.7	15.8
TA_GDU620UL	40.9	29.2	24.0	22.6	20.7	20.1
TA_GDU620UR	47.8	29.0	23.7	21.9	19.7	19.1
TA_GDU620	39.0	25.8	20.7	19.1	17.0	17.8
TA_GTN750	40.1	24.2	19.4	18.2	16.6	15.9
TA_GTR225B	34.9	24.4	18.2	17.0	14.9	15.5
TA_VEMD	43.4	30.4	22.0	20.5	18.4	18.8
TA_MD302	42.3	29.4	23.1	21.4	19.2	19.9
TA_CPA711L	30.6	18.8	13.9	12.7	10.6	12.3
TA_PA711L	30.9	22.4	17.9	16.0	13.6	15.6
TA_WARNPNL	29.4	30.5	N/A	N/A	N/A	N/A

Airbus had also provided engineering design drawings to help create a CAD model of the control panel using SolidWorks. Figures A.1-A.3 in Appendix A were provided by Airbus. Although the drawings were incomplete, a member of the team was able to completely reverse engineer the drawings to create the solid models. The model of the control panel is shown in Figures 1.3 and 1.4.

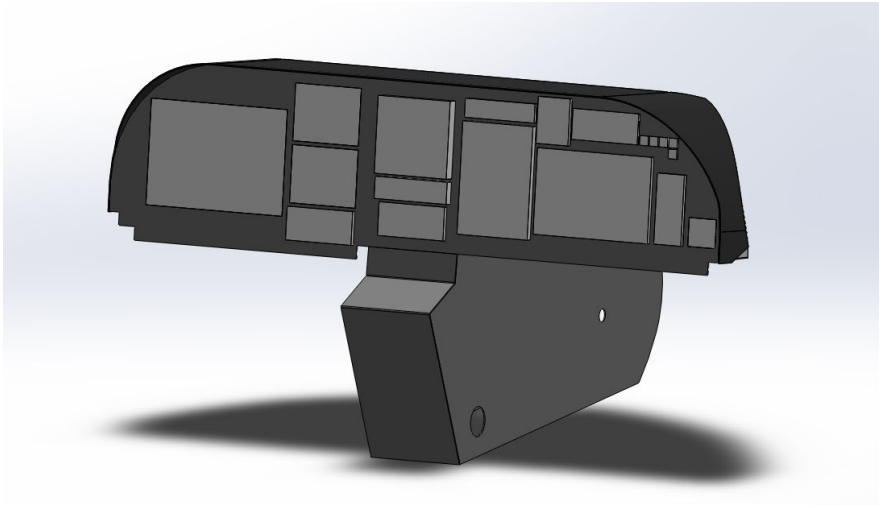

Figure 1.3: Front of Control Panel Model

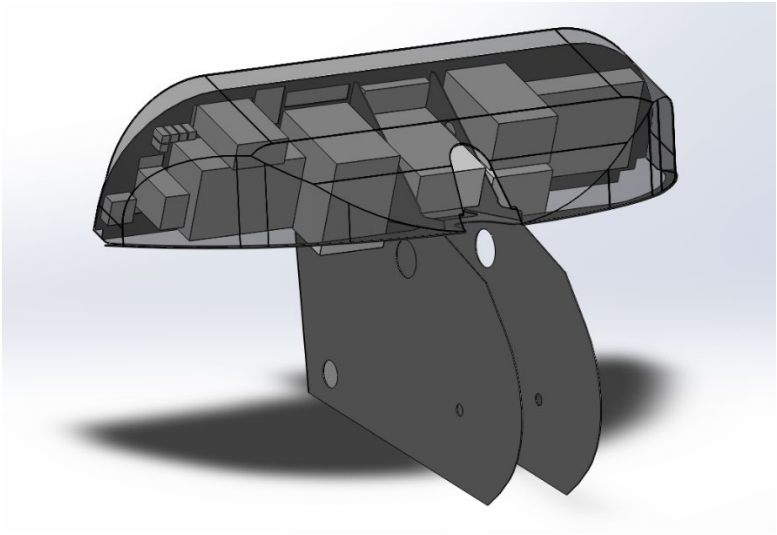

Figure 1.4: Rear of Control Panel Model

1.3 Personal Contributions

This group project required its members to collaborate heavily with each other in order to complete the given tasks. The tasks described hereinafter the conclusion of this section summarizes a majority of my work for the senior design project as well as further contributions not mandated by Airbus and our advisor. Furthermore, references to work performed by other members will be made clear so as to not misappropriate contributions to the completion of the project.

CHAPTER 2

ICEPAK MODEL OF THE CONTROL PANEL

2.1 Icepak Setup

ANSYS Icepak, a computational fluid dynamics (CFD) program, was used to simulate and analyze air flow and thermal conditions of electrical equipment in the control panel. An unideal scenario for thermal conditions, i.e. hovering, was chosen to be replicated in Icepak. This is because the extreme temperatures during hovering may cause failure in the equipment. Figure 2.1 shows the control panel from the front of the helicopter. Note that there are large bulky wires present. This can impede natural airflow and cause hotspots to form around high-power equipment. Figure 2.1 lacks a glare shield while other models do indeed have them. Refer to Figure 1.4 to view the glare shield.

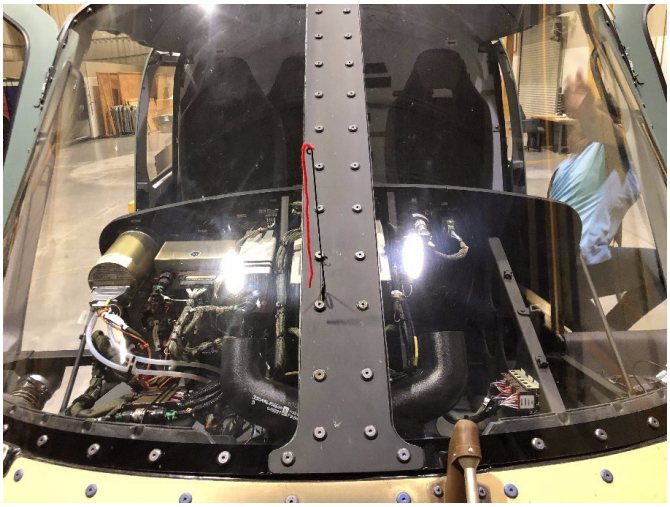

Figure 2.1: Control Panel Viewed from Front of Helicopter

The solid model created by one of the team members was uploaded into ANSYS Workbench, a software for thermal, structural, and electromagnetic analysis, and modified in ANSYS SpaceClaim to prepare the model for Icepak. Each of the equipment's power consumption was extracted from the manuals provided by Airbus. However, since no equipment is ever 100% efficient and/or running constantly, some reasonable modifications were made to the power, which is shown in Table 2.1.

Table 2.1: Equipment Power Consumption

Equipment	Power Consumption (W)
Dimming Control Panel	0.1
Rotor Tachometer	2
LED Annunciator	1.2
Warning Panel Interface	16
Clock	6
Flight Display	42
Navigator	16
Transceiver	7.8
Monitor	12
Standby Altitude Indicator	5
Radio 1	7.8
Radio 2	7.8
Audio Controller	28
Vehicle and Engine Management Display	45

For the control simulations, simulations to reflect the actual helicopter control panel and which will be compared to other simulation results, specific boundary conditions needed to be made. The glare shield and control panel frame can safely be assumed to be blackbody structures. Also, the flow condition was set to buoyancy driven, to allow for natural convection. The mathematical model for natural convection is the Boussinesq approximation, where changes in density are considered minuscule (2). This allows for density to remain constant during the simulations. The flow of the Icepak model

is assumed to be turbulent. If the model is not turbulent, the simulation will adjust for this and solve the model using laminar flow conditions. The zero equation, or algebraic turbulence model, was chosen to perform calculations for the simulation. The zero equation is the simplest of all the turbulence models, which allows for the solution to be calculate directly from the flow variables (3). Finally, heat transfer between surfaces due to radiation was included and the system was assumed to be steady state. The convergence criteria determine when the simulation is finished. Any divergence in the model indicates poor meshing or boundary conditions. The convergence criteria for the velocity vectors and continuity were a loose convergence of $1x10^{-3}$, while the energy values had a tight convergence of $1x10^{-7}$. Different boundary conditions will be chosen for the models various cooling solutions.

2.2 Mesh Quality

The mesh of a CFD model greatly impacts how well the simulation converges. A large mesh with a large element count may be more accurate but will also slow down simulation time. A large portion of this project was focused on this task of optimizing the mesh while trying to avoid errors in the simulations. We were also far more concerned with properly meshing the curved surfaces of the control panel than the prism like structure of the equipment.

Factors such as mesh skewness, volume, and face alignment determined how good the mesh was. Skewness, however, is the most important quality factor. A skewness value of 1 is most ideal. Values close to 0 are said to be completely degenerate as it fails to capture the geometry of the model correctly. A trial-and-error approach by other team members was used to achieve the ideal mesh, which is used as a foundation for all future

Icepak simulations. The mesh parameters that should remain consistent are the global mesh parameters, multi-level parameters, and the miscellaneous parameters. The minimum elements in gap, minimum elements on edge, and the max size ratio, have values of 3 mm, 2 mm, and 2 mm, respectively. Stair-stepped meshing, separate assembly meshes, and average uniform mesh parameters are all enabled. Multi-level meshing is also enabled with a max layer value of 3 mm and a buffer layer of 1 mm. The proximity and curvature size functions should also be enabled. The max element size and minimum gap sizes are changed to increase or lower mesh element count.

2.3 Control Simulation Results

The results of the control simulation are shown in Figure 2.2 and Table 2.2. Figure B.1 in Appendix B shows the convergence plot for the Control model. Note that the errors are very high in some of the equipment temperatures. However, the point of this project is the proof of concept, that is if the cooling methods are successful in lowering the temperature, then implementing them into the control panel may yield similar results.

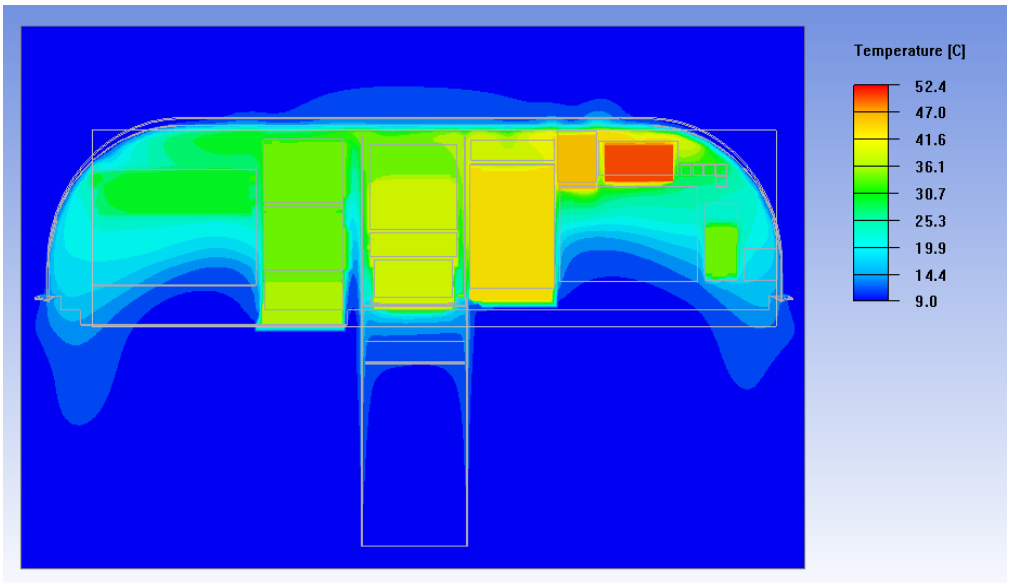

Figure 2.2: Temperature Contour of Control Model

Table 2.2: Experimental Probe Data vs Simulated Probe Data

Electronic Components	Experimental Probe Temps (°C)	Simulated Control Temps (°C)	Error %
OAT	9	9	
TA_CABIN	18.0	9.29328	48.4
TA_MB12W	23.2	21.4231	7.7
TA_IPL	20.5	18.6073	9.2
TA_RADIO1	25.4	33.2721	31.0
TA_RADIO2	21.0	21.7357	3.5
TA_GDU620LL	23.8	19.8269	16.7
TA_GDU620LR	21.0	21.4545	2.2
TA_GDU620UL	29.2	45.9686	57.4
TA_GDU620UR	29.0	31.241	7.7
TA_GTN750 (navigator)	24.2	34.4582	42.4
TA_GTR225B (transceiver)	24.4	15.2538	37.5
TA_VEMD	30.4	37.1793	22.3
TA_MD302 (attitude)	29.4	34.1746	16.2
TA_CPA711L (audio pan)	18.8	20.832	10.8
TA_WARNPNL	30.5	45.7756	50.1

CHAPTER 3

COOLING THE CONTROL PANEL

There are various methods that could be used to cool the control panel. Redirection of air with piping, venting, or fans may achieve proper cooling. The team decided on pursuing two methods: adding perforated holes to the glare shield and adding fans. A member of the team made these changes to the solid models for testing. The perforated holes will act as a grille, which will allow hot air to naturally escape from behind the control panel. Fans will be able to provide high cooling but may just circulate the hot air to another location within the control panel. The sections below will discuss in detail the implementation of these cooling methods in the control panel.

3.1 Perforated Holes

Two separate versions of perforations were added to the glare shield. The first had a localized section above the hottest location within the control panel. The other had perforations that spanned the entirety of the glare shield. Figures 3.1 and 3.2 show these two configurations.

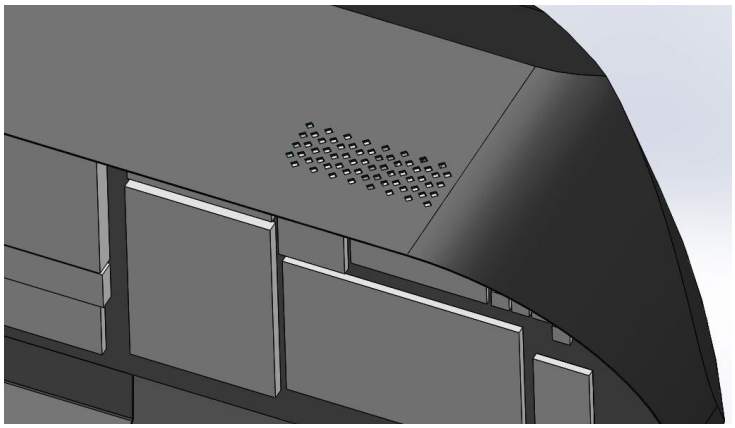

Figure 3.1: Localized Perforations

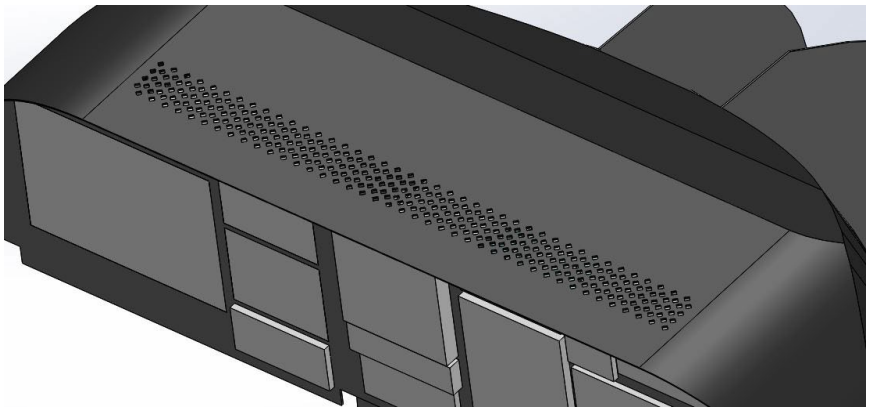

Figure 3.2: Perforations Spanning Glare Shield

3.1.1 Perforated Hole Simulation Results

The boundary conditions for these models are the same as the control model. The meshing parameters are also the same besides the maximum element size and minimum gap size, which will only increase element count. Figures 3.3 and 3.4 show the temperature contour of the control panels with localized and spanning perforations, respectively. Figures B.2 and B.3 in Appendix B show the convergence plots of these two configurations. Tables 3.1 shows the numerical temperature values of each equipment. Table 3.2 shows the difference in the temperature to the control model. As shown in Table 3.2, the model with the perforations that span the glare shield had a higher temperature

difference, therefore it cooled more than the localized perforations. However, the average cooling provided by the spanned perforations is 3.8 °C compared to the localized average cooling of 2.4 °C, which may not make that big of a difference.

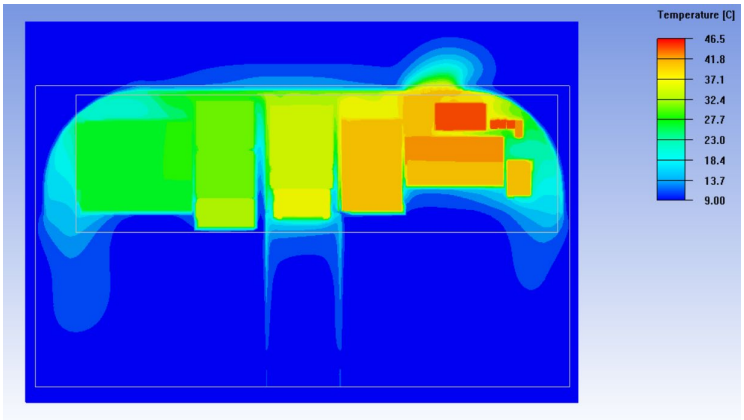

Figure 3.3: Temperature Contour of Localized Perforated Configuration

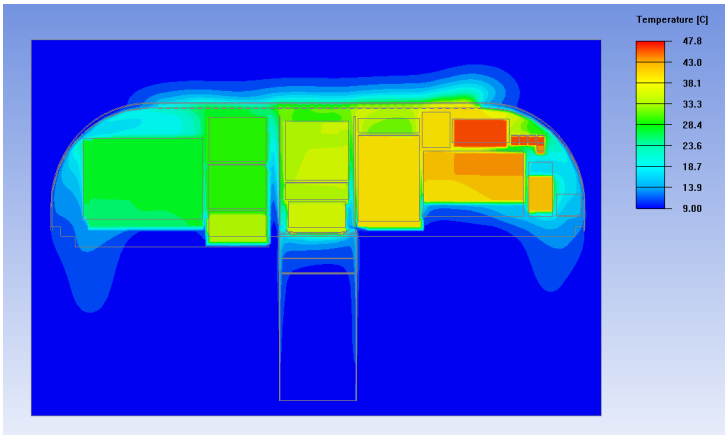

Figure 3.4: Temperature Contour of Spanning Perforated Configuration

Table 3.1: Temperatures of Localized and Spanned Perforations

Electronic Components	Simulated Control Temps (°C)	Localized Perforations Temps	Spanned Perforations Temps
OAT	9.0	9.0	9.0
TA_CABIN	9.3	9.2	9.3
TA_MB12W	21.4	17.9	13.8
TA_IPL	18.6	15.7	12.3
TA_RADIO1	33.3	30.0	30.8
TA_RADIO2	21.7	23.7	23.1
TA_GDU620LL	19.8	17.7	17.2
TA_GDU620LR	21.5	24.0	24.7
TA_GDU620UL	46.0	41.2	41.5
TA_GDU620UR	31.2	27.1	22.2
TA_GTN750	34.5	30.2	25.5
TA_GTR225B	15.3	11.6	11.1
TA_VEMD	37.2	32.5	27.5
TA_MD302	34.2	38.8	37.6
TA_CPA711L	20.8	20.3	20.5
TA_WARNPNL	45.8	35.3	36.0

Table 3.2: Temperature Differences of Localized and Spanned Perforations

Electronic Components	Localized ΔT	Spanned ΔT
OAT	0.0	0.0
TA_CABIN	0.1	0.0
TA_MB12W	3.5	7.6
TA_IPL	2.9	6.3
TA_RADIO1	3.3	2.5
TA_RADIO2	-2.0	-1.3
TA_GDU620LL	2.2	2.6
TA_GDU620LR	-2.5	-3.2
TA_GDU620UL	4.8	4.5
TA_GDU620UR	4.1	9.1
TA_GTN750	4.3	9.0
TA_GTR225B	3.6	4.1
TA_VEMD	4.6	9.7
TA_MD302	-4.6	-3.5
TA_CPA711L	0.6	0.3
TA_WARNPNL	10.4	9.8
Average Cooling:	2.4	3.8

3.2 Fans

Like the perforations, two different configurations of fans are to be simulated. The first is a singular local fan directly above the right side of the control panel, in the same location as the localized hole model. The second model uses three fans that are equally spaced along the length of the glare shield. There are two types of fans, blowing and exhaust fans (4). Exhaust fans draw air from a system while blowing fans push air. The fan chosen for these simulations are a standard aviation vane axial fan from AMETEK Rotron (5). Figures 3.5 and 3.6 show these two configurations with holes cut out for the fans. The fans are inserted into Icepak using the data from Rotron.

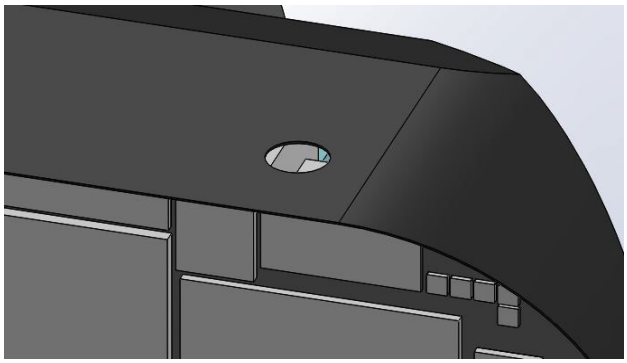

Figure 3.5: Single-Fan Configuration

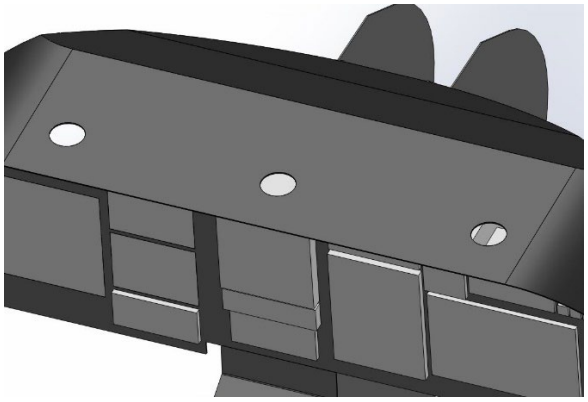

Figure 3.6: Three-Fan Configuration

3.2.1 Fan Simulation Results

The boundary conditions for these are the same as previous models, except that forced convection is enabled in the problem setup. Rather than blow air into the control panel, the fans were used to draw hot air out of the control panel. Figures 3.7 and 3.8 show the temperature contour of the control panels with single and three-fan configurations. Figures 3.9 and 3.10 show the velocity vectors of the air for both fan setups. Figures B.4 and B.5 in Appendix B shows the convergence plots for these simulations. Tables 3.3 shows the numerical temperature values of the equipment for both simulations. Table 3.4 shows the total average cooling for both simulations. As seen in Table 3.4, the three-fan model was much more successful at cooling the control panel than the one fan model. Also, the max temperature present in the three-fan configuration is 39.6 °C compared to the single-fan configuration's 43.3°C.

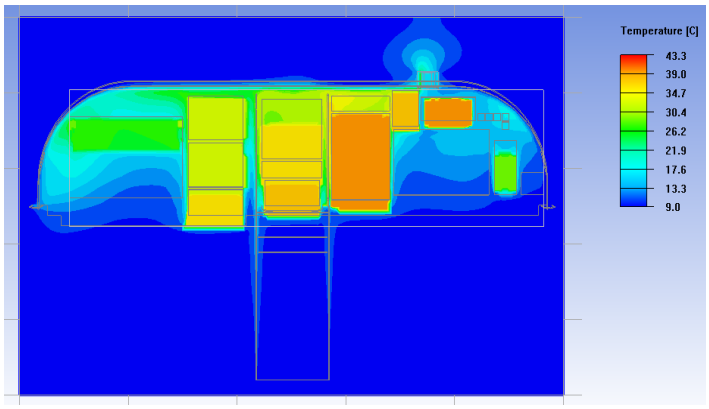

Figure 3.7: Temperature Contour of Single-Fan Configuration

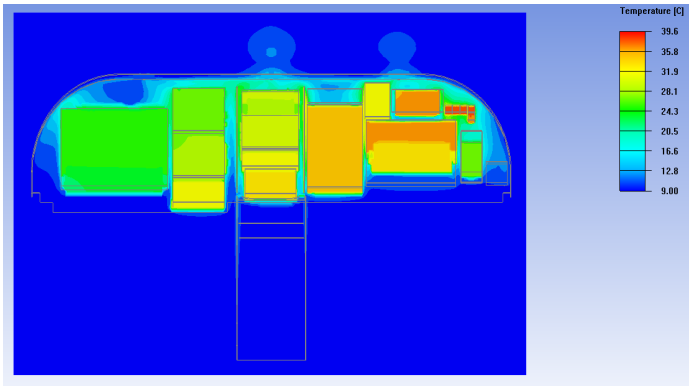

Figure 3.8: Temperature Contour of Three-Fan Configuration

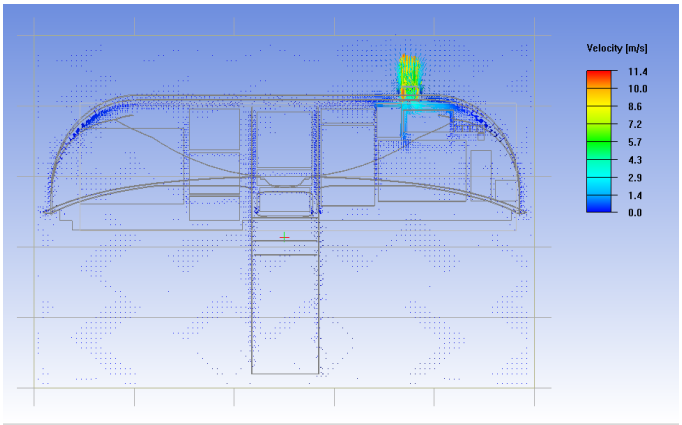

Figure 3.9: Velocity Vector of Single-Fan Configuration

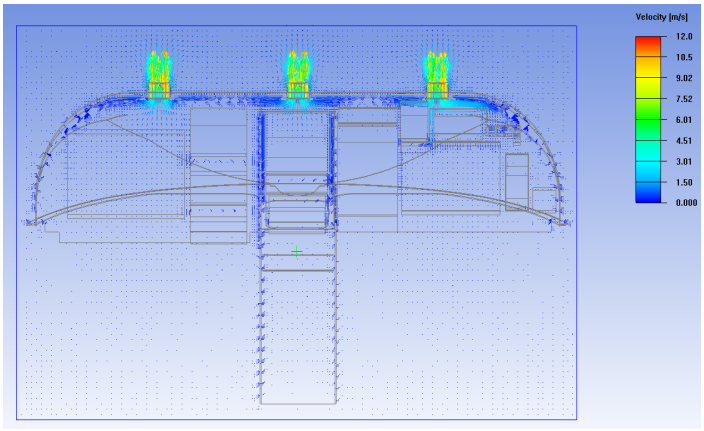

Figure 3.10: Velocity Vectors of Three-Fan Configuration

Table 3.3: Temperatures of Single-Fan and Three-Fan Configurations

Electronic Components	Control Temps (°C)	Single Fan	Three Fans
OAT	9.0	9.0	9.0
TA_CABIN	9.3	9.5	9.0
TA_MB12W	21.4	18.8	11.0
TA_IPL	18.6	15.8	9.6
TA_RADIO1	33.3	27.4	18.7
TA_RADIO2	21.7	19.6	14.4
TA_GDU620LL	19.8	22.0	17.6
TA_GDU620LR	21.5	19.1	16.4
TA_GDU620UL	46.0	38.8	33.3
TA_GDU620UR	31.2	15.6	15.0
TA_GTN750	34.5	27.3	13.3
TA_GTR225B	15.3	14.4	9.9
TA_VEMD	37.2	29.1	11.3
TA_MD302	34.2	30.7	27.8
TA_CPA711L	20.8	18.1	14.7
TA_WARNPNL	45.8	18.9	19.4

Table 3.4: Temperature Differences of Single-Fan and Three-Fan Configurations

Electronic Components	Single Fan ΔT	Three Fans ΔT
OAT	9.0	9.0
TA_CABIN	-0.2	0.3
TA_MB12W	2.6	10.6
TA_IPL	2.8	8.8
TA_RADIO1	5.9	11.6
TA_RADIO2	2.1	4.8
TA_GDU620LL	-2.2	2.1
TA_GDU620LR	2.3	4.2
TA_GDU620UL	7.2	13.5
TA_GDU620UR	15.6	17.3
TA_GTN750	7.2	21.5
TA_GTR225B	0.9	5.7
TA_VEMD	8.1	25.8
TA_MD302	3.5	7.8
TA_CPA711L	2.8	4.3
TA_WARNPNL	26.9	30.1
Average Cooling:	5.7	11.2

3.2.2 Fan Orientation of Three Fan Configuration

The orientation of the fans plays a large role in total cooling in the model. The three-fan configuration was altered so that the two exterior fans blow air into the control panel while the middle fan draws air out. Performing the simulation again with this new orientation provided greater cooling than if the fans all simply pulled air out of the panel area. Figure 3.11 shows the temperature contour of this 'IN/OUT' orientation. Figure 3.12 shows the velocity vectors for this model. The convergence plot is shown in Figure B.6 in Appendix B. Tables 3.5 shows both the temperature of the equipment and the total cooling of the 'IN/OUT' orientation. The max temperature in this new model is 31.8 °C, way below the control max temperature of 52.4 °C.

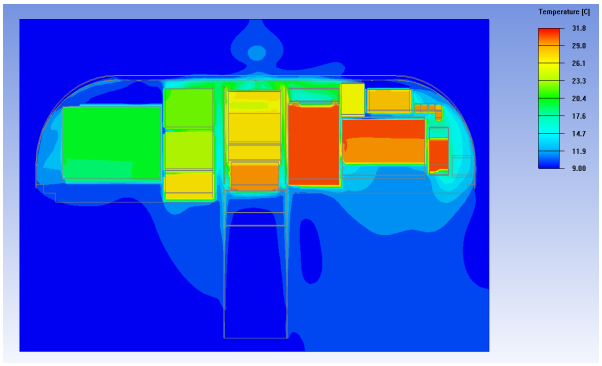

Figure 3.11: Temperature Contour of Three-Fan In/Out Configuration

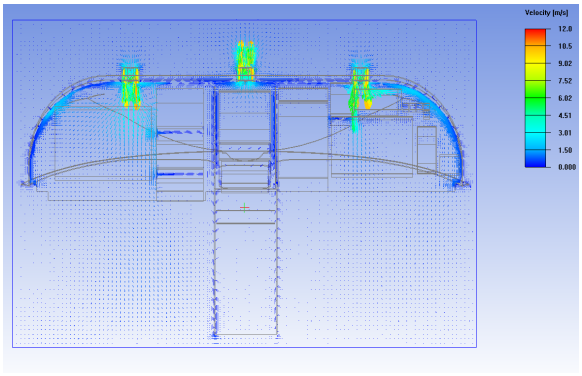

Figure 3.12: Velocity Vectors of Three-Fan In/Out Configuration

Table 3.5: Temperature and Temperature Difference of Three-Fan In/Out Configuration

Electronic Components	Control Temps (°C)	Three-Fan IN/OUT Temps	Three Fans IN/OUT ΔT
OAT	9.0	9.0	0.0
TA_CABIN	9.3	9.0	0.3
TA_MB12W	21.4	11.0	10.4
TA_IPL	18.6	11.8	6.8
TA_RADIO1	33.3	18.5	14.7
TA_RADIO2	21.7	14.6	7.1
TA_GDU620LL	19.8	16.4	3.5
TA_GDU620LR	21.5	16.1	5.3
TA_GDU620UL	46.0	27.0	19.0
TA_GDU620UR	31.2	12.8	18.5
TA_GTN750	34.5	12.1	22.4
TA_GTR225B	15.3	9.7	5.5
TA_VEMD	37.2	11.2	26.0
TA_MD302	34.2	21.5	12.7
TA_CPA711L	20.8	17.3	3.6
TA_WARNPNL	45.8	13.4	32.4
Average Cooling:	N/A	N/A	12.5

3.3 Combination

The combination configuration combines both the perforations and fans into one model. Figure 3.13 shows the model of this configuration. The idea for this model is that both the perforations and fans may provide the best of both natural and forced convection. For the first simulation, all fans were set to pull air out of the control panel interior.

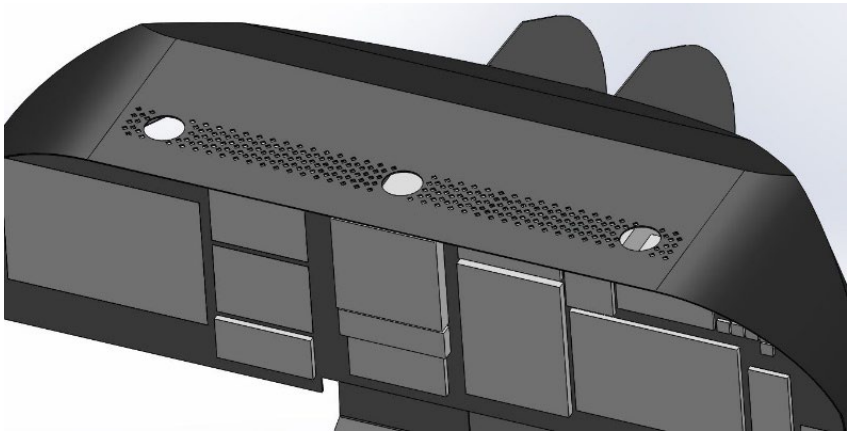

Figure 3.13: Combination Configuration

3.3.1 Combination Simulation Results

The boundary conditions for this configuration are the same as the fan configurations. Figure 3.14 shows the temperature contour of the model and figure 3.15 shows the velocity vectors. Figure B.7 in Appendix B shows the convergence plot. Table 3.6 shows both the temperatures of the equipment and the temperature differences provided by this cooling method.

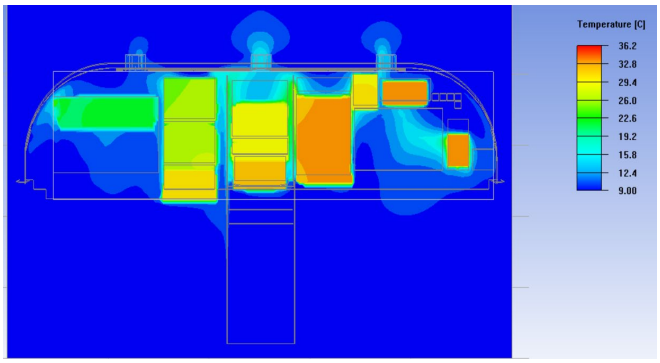

Figure 3.14: Temperature Contour of Combination Configuration

.

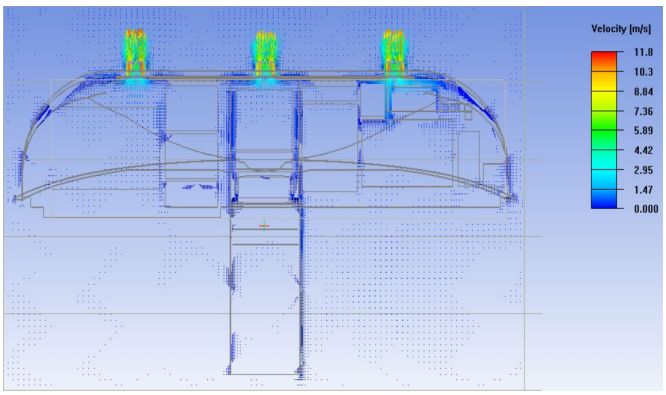

Figure 3.15: Velocity Vectors of Combination Configuration

Table 3.6: Temperature and Temperature Differences of Combination Configuration

Electronic Components	Control Temps (°C)	Combination Temperature	Combination ΔT
OAT	9.0	9.0	9.0
TA_CABIN	9.3	9.0	0.2
TA_MB12W	21.4	10.8	10.6
TA_IPL	18.6	9.6	9.0
TA_RADIO1	33.3	18.3	11.4
TA_RADIO2	21.7	15.6	4.3
TA_GDU620LL	19.8	17.5	2.0
TA_GDU620LR	21.5	16.3	4.1
TA_GDU620UL	46.0	33.3	12.9
TA_GDU620UR	31.2	15.1	17.1
TA_GTN750	34.5	13.4	21.3
TA_GTR225B	15.3	9.8	5.6
TA_VEMD	37.2	12.1	25.1
TA_MD302	34.2	27.8	7.0
TA_CPA711L	20.8	14.6	4.3
TA_WARNPNL	45.8	18.7	29.9
Average Cooling:	N/A	N/A	11.0

3.3.2 Fan Orientation of Combination Configuration

Similar to the section 3.2.2, the fan orientation will be modified so that the exterior fans are blowing air into the control panel and the middle fan draws hot air out. Figure 3.16 shows the temperature contour of this fan orientation. Figure 3.17 shows the velocity vectors of the model. Note that max temperature is 31.5 °C, roughly 5 degrees lower than if all fans were drawing air out. Table 3.8 shows both the equipment temperatures and the average cooling the system provides. Figure B.8 in Appendix B shows the convergence plot for this configuration.

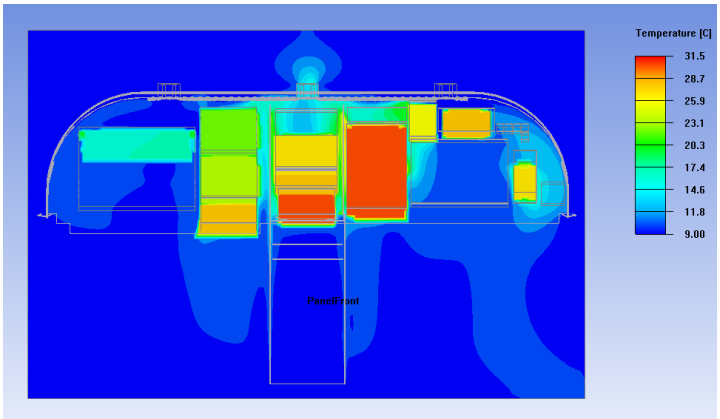

Figure 3.16: Temperature Contour of Combination In/Out Configuration

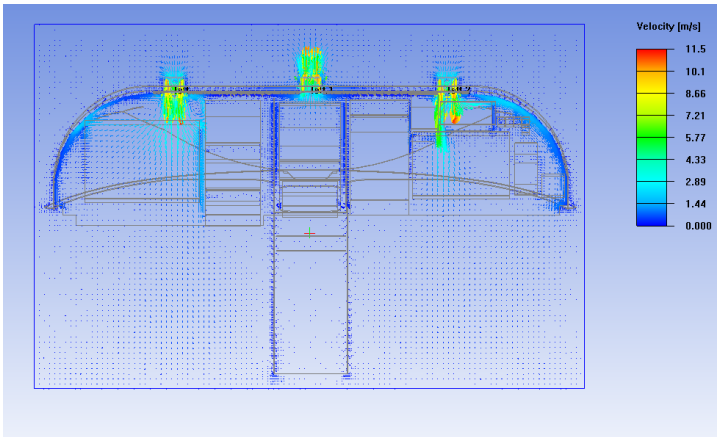

Figure 3.17: Velocity Vectors of Combination In/Out Configuration

Table 3.7: Temperature and Temperature Differences of Combination In/Out Configuration

Electronic Components	Control Temps (°C)	Combo IN/OUT	Combo IN/OUT ΔT
OAT	9.0	9.0	0.0
TA_CABIN	9.3	9.0	0.3
TA_MB12W	21.4	10.5	10.9
TA_IPL	18.6	10.8	7.8
TA_RADIO1	33.3	16.0	17.2
TA_RADIO2	21.7	10.7	11.0
TA_GDU620LL	19.8	16.6	3.2
TA_GDU620LR	21.5	13.5	8.0
TA_GDU620UL	46.0	26.9	19.1
TA_GDU620UR	31.2	11.7	19.5
TA_GTN750	34.5	12.0	22.5
TA_GTR225B	15.3	10.3	5.0
TA_VEMD	37.2	11.3	25.8
TA_MD302	34.2	27.0	7.2
TA_CPA711L	20.8	15.4	5.4
TA_WARNPNL	45.8	15.6	30.2
Average Cooling:	N/A	N/A	12.9

CHAPTER 4

CONCLUSIONS & RECOMMENDATIONS

Each of the cooling solutions were successful in reducing internal air temperatures and was able to reduce maximum air temperature within the control panel. However, the primary goal of the project is to create a method that provides the most cooling to the panel instrumentation. Upon completion and analysis of the data, it can confidently be said that the three-fan in/out and combination in/out configurations both provided excellent cooling to the control panel. This was somewhat expected as fan systems generally provide greater cooling when compared to a simple grille.

Total cooling of a fan system is heavily dependent on the fan orientation. By modifying the orientation of the fans, the total achievable cooling can be drastically increased compared to if all fans were oriented the same. In three-fan in/out and combination in/out configurations, maximum temperatures dropped by approximately 22 °C. It can be expected that by implementing one of these solutions into the Airbus H125 helicopter control panel will yield similar results. However, strictly comparing these two solutions, the perforations in the combination configuration seem mostly unnecessary since both the three-fan and combination configurations achieve similar values. It can thus be safely given that the three-fan in/out configuration should have the highest recommendation for implementation into the control panel.

APPENDIX A

AIRBUS INSTRUMENT PANEL LAYOUT AND DRAWINGS

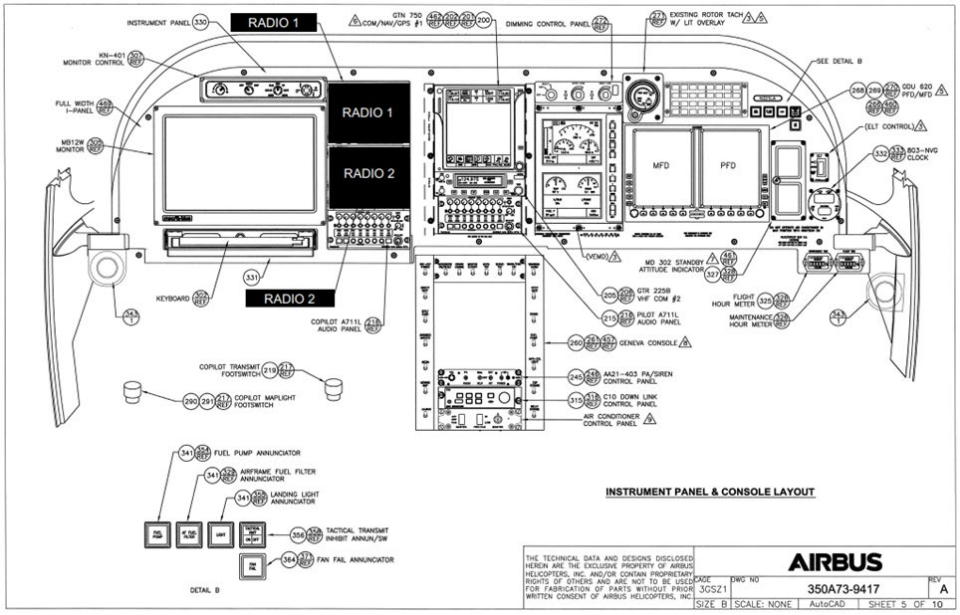

Figure A.1: Instrument Panel and Console Layout

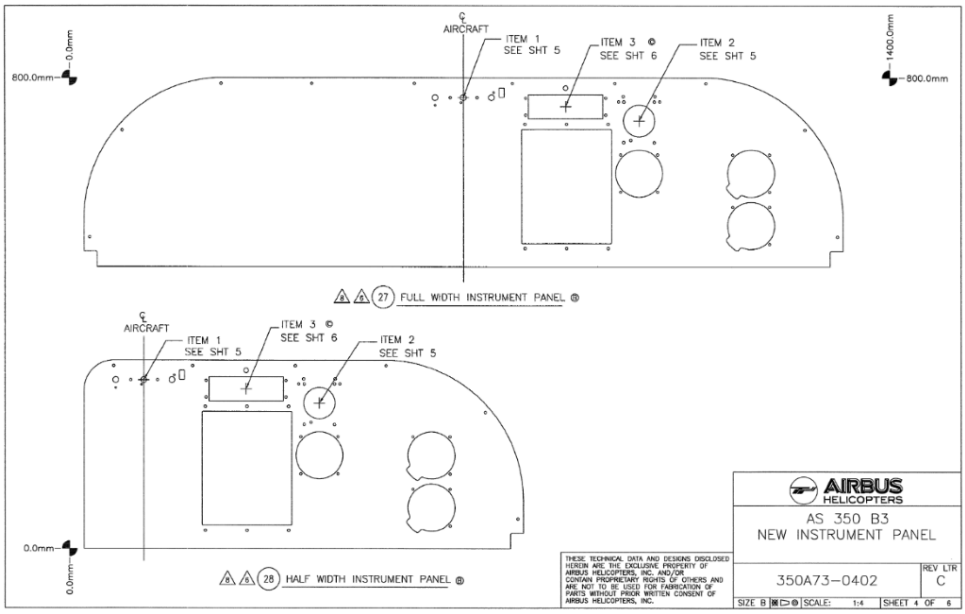

Figure A.2: Instrument Panel Drawing

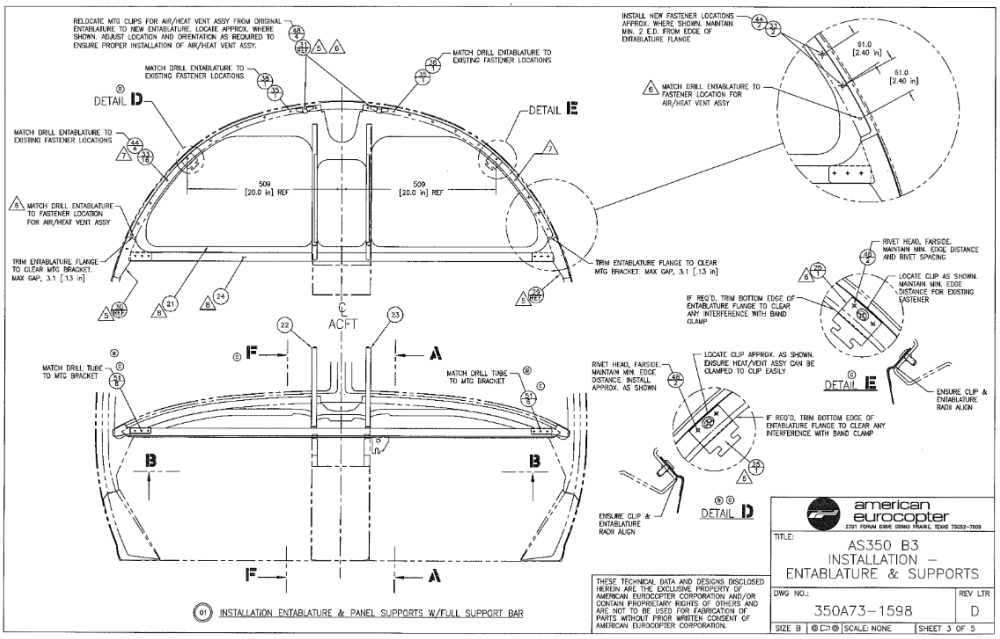

Figure A.3: Control Panel Support Structure

APPENDIX B

CONVERGENCE PLOTS

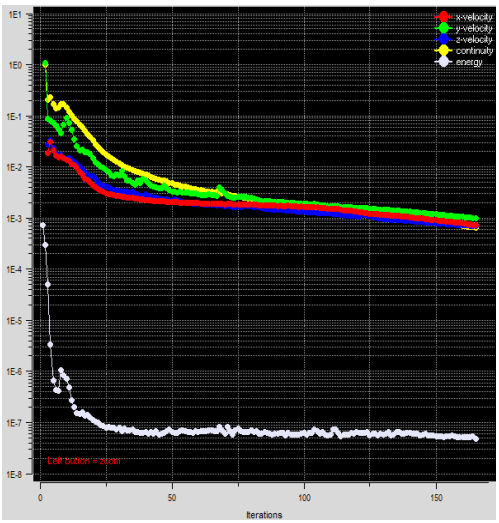

Figure B.1: Convergence Plot for Control

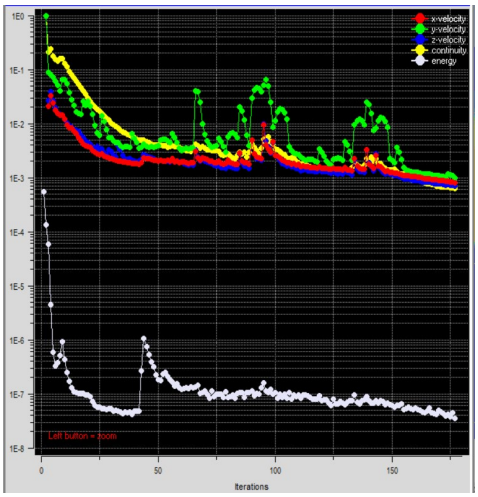

Figure B.2: Convergence Plot for Localized Perforations

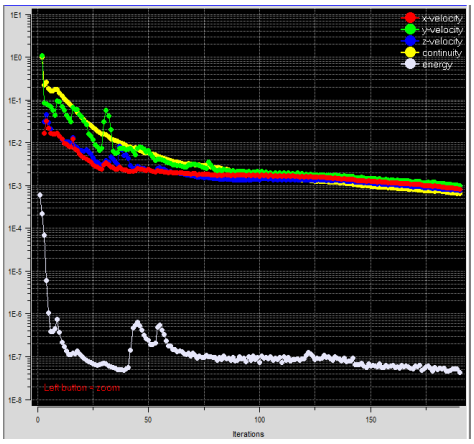

Figure B.3: Convergence Plot for Spanning Perforations

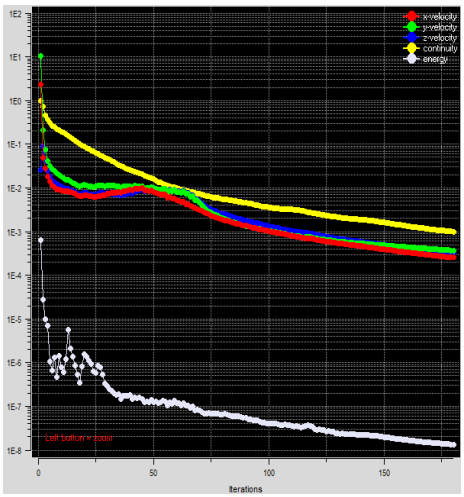

Figure B.4: Convergence Plot for Single-Fan Configuration

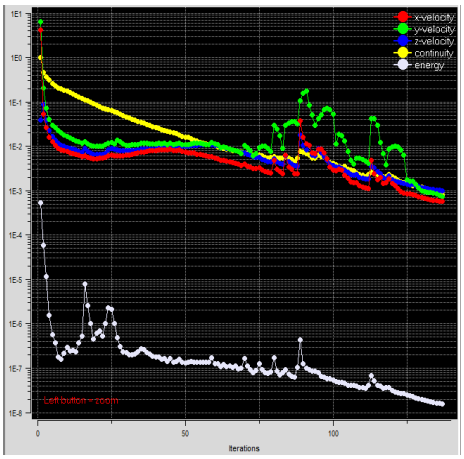

Figure B.5: Convergence Plot for Three-Fan Configuration

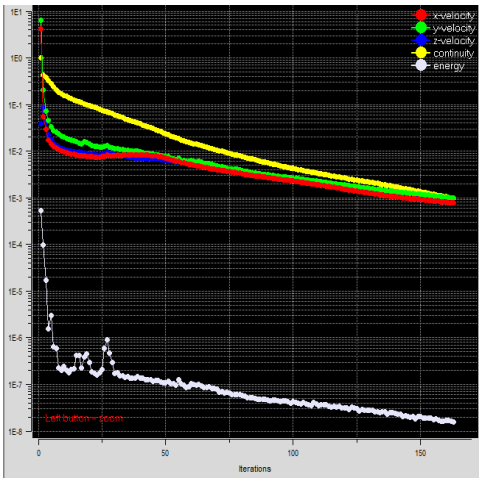

Figure B.6: Convergence Plot for Three-Fan In/Out Configuration

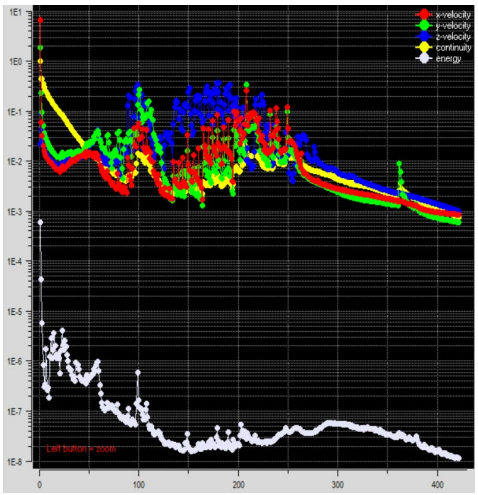

Figure B.7: Convergence Plot for Combination Configuration

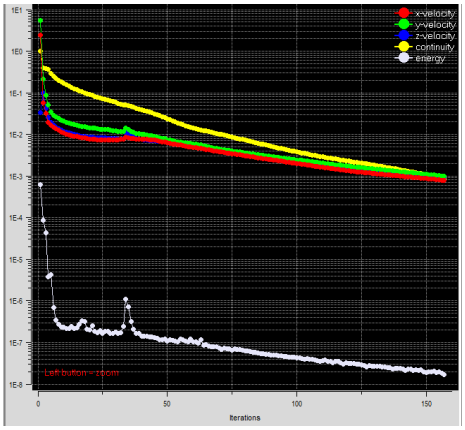

Figure B.8: Convergence Plot for Combination In/Out Configuration

REFERENCES

[1] Airbus, *H125M rapid response, 2010*

[2] Hansen, J., , *Fluid Dynamics of the Atmosphere and Ocean: Lecture 7,* 2004, Massachusetts Institute of Technology, MIT Open Courseware

[3] CFD Online, *Algebraic turbulence models, 2007*

[4] AMETEK Rotron, *Rotron AXIMAX 2 Small Vaneaxial Fans*

[5] Steinberg, D. S., *Force-Air Cooling for Electronics*: *In Cooling Techniques for Electronic Equipment*, John Wiley & Sons, Inc., 2nd ed., pp. 157–202

BIOGRAPHICAL INFORMATION

Cristobal Garces will be a University of Texas at Arlington (UTA) graduate at the conclusion of the Spring 2020 semester. He will be receiving his Honors Bachelor of Science in Mechanical Engineering with a minor in Physics. Cristobal has participated in undergraduate research with the Physics Department with Dr. Jaehoon Yu. He has made contributions to the international project known as the Deep Underground Neutrino Experiment during his time at UTA. Cristobal has also contributed to the Short Baseline Neutrino Detector during his stay at Fermilab National Laboratory located in Batavia, Illinois. Cristobal plans to pursue a PhD in Aerospace or Mechanical Engineering, though has yet to decide where he will attend.